

Comparative structural evaluation of serial X-ray free electron laser and electron crystallography

Single-crystal X-ray diffraction (SCXRD) is the most common method used to resolve crystal structures experimentally. The structure determination requires a sufficient crystal size, typically larger than 100 μm , based on the atomic cross-section and the flux of probing photons. However, developments in microcrystallography since the 2010s have introduced alternative approaches to overcome the limitations of conventional methods. Three-dimensional electron diffraction (3D ED/ED, [1,2]) has emerged as a powerful technique capable of resolving structures from crystals that are too small for SCXRD, owing to the larger atomic cross-section of electrons (X-ray, $\sim 10^0 - 10^1$ barns; electron, $\sim 10^5$ barns [3]). On the other hand, X-ray free electron lasers (XFELs) provide another solution through serial X-ray crystallography with femtosecond pulses (SX/SFX, [4]), allowing the measurement of large numbers of small crystals with intense pulsed photons ($\sim 10^{12}$ photons/pulse). These techniques are not alternatives to each other but offer specific insights into crystal structures owing to the distinct features of the interaction between probes and targets. X-rays scatter through interactions with electrons, whereas electrons scatter through Coulomb potentials. Electrons are more sensitive to atomic charges than X-rays [2], particularly because of the positive charge contribution of the core protons (Fig. 1). However, to date, no direct or quantitative assessments of ED and SX have been performed. In our study, we applied both ED and SX methods to the same target, microcrystals of rhodamine-6G, and compared the obtained structures at a subatomic resolution [5].

We developed a fixed-type data collection system at SACLA BL2 for the SX measurement of small compounds. The microcrystals were dispersed on a

flat-faced polyimide plate, and the plate was moved in 2D directions as scanned by the XFEL beam at room temperature (r.t.). Serial diffraction patterns were recorded using a CCD camera synchronized with the pulse repetition at 30 Hz. A higher photon energy of 15.0 keV and a shorter camera distance (100 mm) enabled the recording of higher-order diffraction. We collected 265,254 frames in 2.5 h and processed them, successfully determining the crystal structure of rhodamine-6G at a resolution of 0.82 \AA using the *ab initio* method.

ED measurements were performed using a CRYO ARM 300 electron microscope at the RIKEN SPring-8 Center. Microcrystals from the same batch used in the SX were spread over a carbon film covering a copper grid. An electron beam accelerated at 300 kV illuminated the individual crystal grains on the grid. Diffraction patterns were recorded on a direct detection detector while rotating the sample stage at r.t. and cryogenic (~ 98 K) specimen temperature. For a detailed comparison with SX, 23 rotation series were selected for the r.t. dataset. The processed and merged datasets of ED also determined the crystal structure at a resolution of 0.90 \AA , revealing that the data quality was superior in the r.t. dataset compared with the cryogenic dataset.

The structures obtained using SX and ED were quantitatively compared. While the configurations of the non-hydrogen atoms are almost identical, the geometric errors in the SX structure are two to five times smaller than those in the ED structure. Hydrogen atoms were visualized in both structures and the differences in their resolved positions were distinguishable (Fig. 2). These dispositions originate from the polarity of the covalent bonds with the

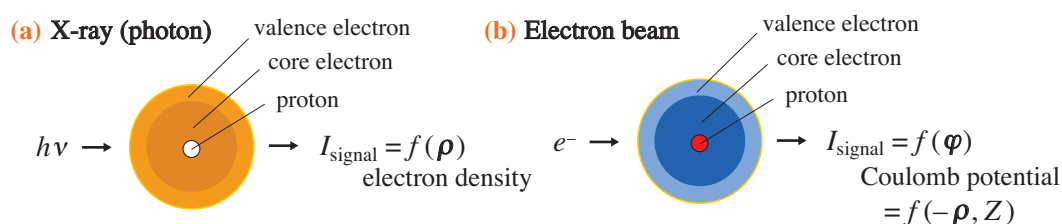


Fig. 1. Interaction of probes with atoms. (a) X-rays scatter through the electrons of the target, and the structure is resolved as electron density (ρ). (b) Electrons scatter through the Coulomb potentials (φ) of the target. While the valence electron is minor component of electron density, that in Coulomb potentials can be more dominant owing to the contribution of the positive charges of proton(s) (Z).

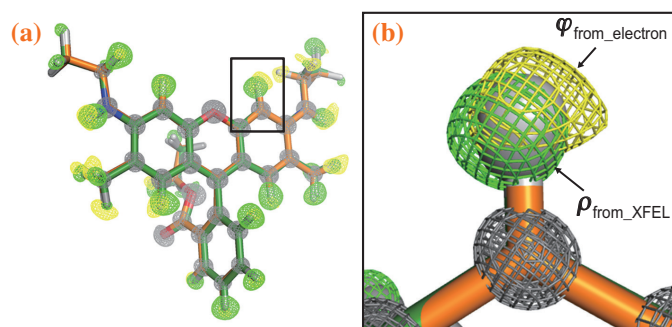


Fig. 2. Hydrogen atoms in rhodamine-6G microcrystal observed with ED and SX. Two types of densities, Coulomb potential (φ , yellow) and electron density (ρ , green), are superimposed for the entire molecule in (a), and a zoomed in view for an aromatic C–H bond in (b). Both densities for non-hydrogen atoms are colored in gray.

hydrogen atoms. We evaluated the sensitivity to the charges of the hydrogen atoms using both methods. The optimal charge values for the two hydrogen atoms at the dissociable sites could be determined by accounting for the measured diffraction intensities of ED, whereas no specific values were obtained from those of SX (Fig. 3). The charge distribution on rhodamine-6G means indicates that a positive charge is not localized but is partially shared with the two interaction sites.

Although the application of SX has been limited to macromolecular crystallography until recently, we demonstrated its potential utility in the structural chemistry of small compounds, enabling direct comparison with the micro-crystallography of ED. These two distinctive techniques can reveal particular features of atomic and subatomic structures in microcrystals, and we expect that they will support the detailed understanding and design of functional molecules further.

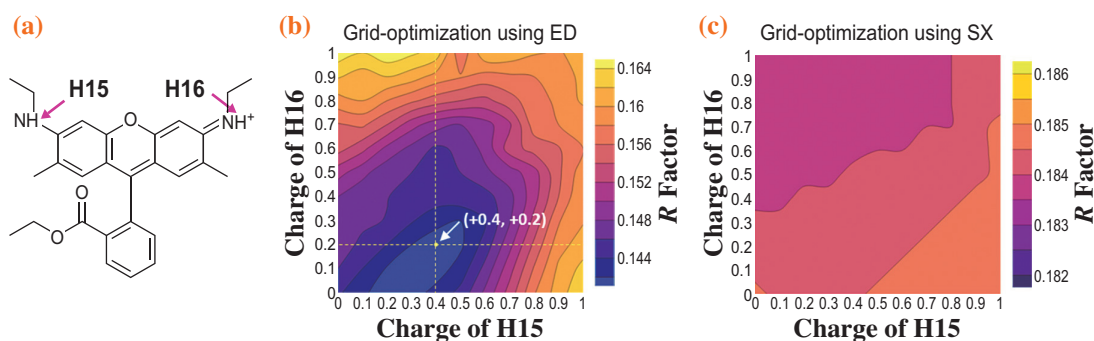


Fig. 3. Atomic charge optimization on rhodamine-6G with ED and SX. (a) Chemical formula of rhodamine-6G. Either of two amide hydrogen atoms (H15 and H16) are only denoted as charged, whereas both of them can be charged partially. (b, c) Diagrams of R values, indicating the discrepancy between the modeled and measured diffraction intensity. The charge values of H15 and H16 are varied along the horizontal and vertical axes. A point indicating the lowest R value in (b), using ED data, indicates the optimal pair of charge values, whereas no point can be observed in (c) using SX data.

Kiyofumi Takaba[†]

RIKEN SPring-8 Center

Email: kiyofumi.takaba@univie.ac.at

[†]Present address: University of Vienna

References

- [1] D. Zhang *et al.*: Z. Kristallogr. **225** (2010) 94.
- [2] K. Yonekura *et al.*: Proc. Natl. Acad. Sci. USA **112** (2015) 3368.
- [3] R. Henderson: Q. Rev. Biophys. **28** (1995) 171.
- [4] H. N. Chapman *et al.*: Nature **470** (2011) 73.
- [5] K. Takaba, S. Maki-Yonekura, I. Inoue, K. Tono, T. Hamaguchi, K. Kawakami, H. Naitow, T. Ishikawa, M. Yabashi and K. Yonekura: Nat. Chem. **15** (2023) 491.